Journal of Geoscience and Environment Protection, 2024, 12, 62-79
https://www.scirp.org/journal/gep
ISSN Online: 2327-4344
ISSN Print: 2327-4336

Using TiO_2-Biocharcoal and TiO_2-Diatomite for Photodisinfection in Washing Machine Wastewater

Daphne Montesuma Ferro[1], Paloma Otsuka Kotani[1], Regina Affonso[2], Nilce Ortiz[1]

[1]Chemistry and Environment Center, Nuclear and Energy Research Institute, IPEN, São Paulo, Brazil
[2]Biotechnology Center, Nuclear and Energy Research Institute, IPEN, São Paulo, Brazil
Email: nortizbr@gmail.com

How to cite this paper: Ferro, D. M., Kotani, P. O., Affonso, R., & Ortiz, N. (2024). Using TiO_2-Biocharcoal and TiO_2-Diatomite for Photodisinfection in Washing Machine Wastewater. *Journal of Geoscience and Environment Protection, 12,* 62-79.
https://doi.org/10.4236/gep.2024.128004

Received: May 2, 2024
Accepted: August 6, 2024
Published: August 9, 2024

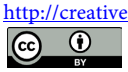

Abstract

The photodisinfection process using biomolded semiconductor photocatalysts can inactivate bacteria in wastewater washing machine samples. The comparative study evaluated the photocatalyst material titanium dioxide (TiO_2) synthesized with diatomite and biocharcoal biotemplate (TiO_2-Biocharcoal and TiO_2-Diatomite) in photodisinfection processes using domestic washing machine wastewater samples, the results of bacterial inactivation were above 96%. The efficiency of the photodisinfection process was evaluated by counting the number of colonies of the bacteria. Experiments under LED solar lamps presented similar bacterial inactivation, and a correlation with kinetic models. The kinetic study demonstrated a curved regression, indicating a better fit with the Hom model. A tail at the end of the modeling curve indicates the presence of a high concentration of inactive bacteria in the medium, while a shoulder at the beginning of the curve suggests a heterogeneous sample with a high concentration of gram-positive bacteria. The toxicity tests performed with wastewater samples without light exposure indicated low toxicity for both materials. The study presented promising disinfection results for an accessible and efficient photo-sterilization process of water contaminated with bacteria using abundant solar and renewable energy throughout the national territory.

Keywords

Photodisinfection, Diatomite, Biocharcoal, Wastewater, Titanium Dioxide

1. Introduction

Water disinfection using sustainable treatment is paramount since traditional

chemical disinfection methods have severe environmental drawbacks, such as the formation of toxic disinfection by-products (DBPs) causing several diseases (Gopal et al., 2007). In addition, the increased weather and climate extreme events reduced water security. The Intergovernmental Panel on Climate Change (IPCC, 2023) 2023 report presented the possibility of prolonged droughts and floods, directly impacting water capture and supply. These events can also affect public health by increasing the incidence of waterborne diseases, such as diarrhea and dysentery (Levy et al., 2018; IPCC, 2023).

Since 2016 Brazil committed to the ONU 2030 Agenda, which includes 17 Sustainable Development Goals (SDG). These goals involve implementing sustainable solutions to ensure health, clean water, and sanitation (UNDG, 2016). Approximately 15 million people live in urban areas without safe water in Brazil. In rural areas, 25 million people have access only to basic water safety levels. Additionally, for 2.3 million people, the water available for drinking and personal hygiene lacks treatment (UNICEF & WHO, 2021). Therefore, the development of affordable and sustainable water treatment becomes necessary.

The application of the widely reported heterogeneous photocatalysis with titanium dioxide (TiO_2) as a semiconductor is due to its accessibility and high photocatalytic activity in anatase form (Wang et al., 2012). In the irradiation of TiO_2 particles by UV light, the conduction band electron jumps to the valence band and forms the electron-hole pairs promoting the formation of reactive oxygen species (ROS) responsible for the microorganism's inactivation (Ortiz et al., 2018; Shimizu et al., 2019).

The photocatalyst efficiency is related to optimizing electron-hole recombination and surface properties to improve photon absorption and intensify reaction kinetics (Fawzi et al., 2022). Diatomite powder is an attractive semiconductor support due to its enhanced surface area and homogeneous pores (Chen et al., 2019). The formation of the structure of diatomite was by the accumulation of small frustules (cell walls or outer layers) of diatom algae, and its main chemical component is amorphous silica (SiO_2) (Wu et al., 2019).

Biochar is a material made by pyrolysis of biomass. It is mostly composed of carbon, and during thermal degradation the porosity increases greatly, also increasing the surface area, this characteristic facilitates the exchange of loads (Trazzi et al., 2018). Micronized biochar acts as a biotemplate and contributes to the synergistic effect, multiplying the results of photodisinfection (Mesones et al., 2020).

Since the pioneering study by Matsunaga et al. (1985), many researchers investigated the utilization of semiconductor photocatalysis for inactivating many pathogenic microorganisms (Coleman et al., 2005; Ortega-Gómez et al., 2013). Among these studies, the most extensively reported investigations revolve around the bactericidal effects of TiO_2 photocatalysis on the inactivation of *E. coli* suspensions (Marugán et al., 2008; Shimizu et al., 2019). Additionally, several studies have specifically examined the influence of photocatalytic process parameters, such as light intensity and TiO_2 concentration (Ganguly et al., 2018;

Marugán et al., 2011). However, few studies have reported bacterial inactivation on real wastewater samples.

Washing machines can clean clothes but don't sterilize and inactivate microorganisms (Callewaert et al., 2015), and those contaminated wastewater goes to the domestic sewerage system and possibly to the water resources. Researchers investigated such greywater samples and found a heterogeneous medium with gram-positive and gram-negative bacteria (Gattlen et al., 2010). The gram-negative bacteria present a more complex cell wall due to multiple layers in its composition, such as the outer membrane, combined with the peptidoglycan layer. On the other hand, the gram-positive bacteria have a thicker cell wall due to the higher thickness of the peptidoglycan layer, this characteristic makes them mechanically more rigid than gram-negative bacteria (Tortora et al., 2016).

The project developed and improved the bacterial inactivation process using solar radiation on contaminated greywater samples collected on domestic washing machines. The comparative processes used 0.5 $g \cdot L^{-1}$ of TiO_2-Diatomite (DT), 0.5 $g \cdot L^{-1}$ of TiO_2-Biocharcoal (BC) and determined the photodisinfection kinetics model.

2. Methods

2.1. TiO_2-Diatomite and TiO_2-Biocharcoal Synthesis and Characterization

The TiO_2-Diatomite was prepared by sol-gel method mixing 10 mL of titanium isopropoxide and 0.125 $mg \cdot mL^{-1}$ of commercial diatomite in nature. Mixing the final suspension for 2 hours, and after 1 hour of settling, the formed solid was in the oven at 100˚C for 24 hours to obtain TiO_2-shaped microstructures. After drying, the disaggregation of the material was manually and sieved (0.60 mm). The synthesized powder characterization analyses used the TiO_2-Diatomite material prepared with 0.125 $mg \cdot mL^{-1}$ of diatomite.

The TiO_2 synthesis by the sol-gel process used 10 mL of titanium isopropoxide and 0.125 $mg \cdot mL^{-1}$ of Biocharcoal powder. The acid hydrolysis lasted 2 hours, and after 16 hours of settling the material was placed in the oven for 5 hours at 100˚C. The synthesized powder characterization analyses used the TiO_2-Biocharcoal material prepared with 0.125 $mg \cdot mL^{-1}$ of biocharcoal.

The best formulation of the photodisinfection experiments used 0.5 $g \cdot 100mL^{-1}$ of TiO_2-Biocharcoal and TiO_2-Diatomite.

The analyses of Scanning Electron Microscopy (SEM) and Brunauer-Teller-Emmett (BET) were in the Materials Characterization Laboratory (LCT) at the Polytechnic School, University of São Paulo (USP). For SEM analysis, the application of carbon coating (graphite) ensured the passage of current and the production of secondary electrons used for image formation.

The samples prepared to determine the surface area of the TiO_2-Diatomite, and TiO_2-Biocharcoal materials by BET used the equipment at 150˚C for degassing and used the Nitrogen gas at 77 K with a pressure variation ranging from

35.88 to 143.65 mmHg and an equilibrium time of 5 seconds for both samples. The mass of the TiO_2-Diatomite sample analyzed was 0.2735 g, and for the TiO_2-Biocharcoal sample, it was 0.6348 g.

In the thermogravimetric analysis (TG-DTA), the sample mass was measured as a function of temperature and time under controlled heating conditions with either nitrogen (N_2) or oxygen (O_2) as the inert or oxidizing gas, respectively, at a flow rate of 40 $mL \cdot min^{-1}$ to 60 $mL \cdot min^{-1}$. The analysis was conducted at the Analytical Center of the Institute of Chemistry (IQ), University of São Paulo (USP), using 13.279 mg of synthesized TiO_2-Diatomite, 8.870 mg of TiO_2-Biocharcoal and the temperature varied from 10˚C to 900˚C.

X-ray diffractometry is a technique used to verify the crystalline structure of a compound. TiO_2 can be found in more than one crystalline form, which can be Anatase, Rutile and Bruquite. The analysis was carried out in equipment that uses a stationary copper (Cu) tube as an X-ray source (30 kV, 15 mA), under the angle 2θ (2 theta), conducted at the Analytical Center of the Institute of Chemistry (IQ), University of São Paulo (USP).

2.2. Photodisinfection Process

The collection of the greywater samples was from a domestic washing machine after the rinse step. The lather step used different types of clothes but only neutral soap addition. The dilution of the collected samples was with 0.9% NaCl and installed in the refrigerator for sample conservancy.

The photoreactor built in the Institute has an Erlenmeyer used for the wastewater sample and the addition of the synthesized material, all set closed with sterilized cotton in the upper part. The cover doesn't interfere with the oxygen transference during the experiments. The reactor promotes the experiments in a controlled environment inside a solar chamber. The LED lamps were installed inside the chamber.

The total process time of all experiments was 60 minutes. The first aliquot collection (time: 0) of all experiments was before radiation exposure, and then the reactor was exposed to radiation with the subsequent collection every 15 minutes. During all processes, the pH range was between 5.0 and 5.5, with the addition of 0.5 $g \cdot L^{-1}$ TiO_2-Diatomite or 0.5 $g \cdot L^{-1}$ of TiO_2-Biocharcoal in the reactors.

The toxicity tests lasted 60 minutes and were carried out in the solar chamber without exposure to light with all parameters controlled. For the process to correlate with the photodisinfection test, the wastewater and 0.5 $g \cdot L^{-1}$ of the synthesized photocatalyst were added to the reactor. The collection of aliquots of the suspension began at minute 0 before the reaction, and the remaining collections were at minutes 15, 30, 45 and 60 of agitation.

The preparation of Agar Luria-Bertani (LB) nutrient cultures was for Petri plates (90 × 15 mm) used to assess the number of bacterial colonies in each collected aliquot. All collections were at sterilized laminar flow hood, and 20 μL of the sampled solution taken at different exposure times was spread on the LB

surface, followed by the addition of 20 µL of saline solution (0.9% NaCl). After the complete aliquots collections, the Petri dishes incubation was at 37˚C for 16 hours.

The bacterial counting (CFU) of bacterial colonies observed in different times were conducted through high-resolution photography, processed using the "GIMP" software, and analyzed with OpenCFU software (Geissmann, 2013). For bacterial counts and kinetic calculations 6 samples of photodisinfection (Table 1) and 6 samples of toxicity tests (Table 2) were selected for this work.

Table 1. Photodisinfection experiments parameters.

Experiment Identification	Radiation	Dilution Proportion (0.9% NaCl)	Temperature (˚C)
1DT	LED	1:10	23.50
2DT	LED	1:100	22.90
3DT	LED	1:100	23.00
1BC	LED	1:20	20.60
2BC	LED	1:20	23.60
3BC	LED	1:20	25.80

(DT: Diatomite; BC: Biochar).

Table 2. Toxicity experiments parameters.

Experiment Identification	Radiation	Dilution Proportion (0.9% NaCl)	Temperature (˚C)
1DT tox	-	1:10	23.00
2DT tox	-	1:100	21.00
3DT tox	-	1:100	21.00
1BC tox	-	1:20	24.10
2BC tox	-	1:20	22.50
3BC tox	-	1:20	25.70

(DT: Diatomite; BC: Biochar).

3. Results and Discussion

3.1. TiO_2-Diatomite Characterization

The synthesized TiO_2-diatomite material presented a final mass ranging from 2.5 g to 3 g. The results of the BET analysis revealed that pure diatomite has a surface area of 6.47 $m^2 \cdot g^{-1}$, while the TiO_2-Diatomite material exhibited a surface area of 216 $m^2 \cdot g^{-1}$. This surface area is four times larger than commercially available TiO_2 for photocatalytic processes (Bianchi et al., 2015).

The SEM micrograph revealed the structure of the synthesized material with uniformly sized and distributed pores, resembling the structure of diatomite. The pores exhibited diameters ranging from 2.5 to 3.8 µm (Figure 1).

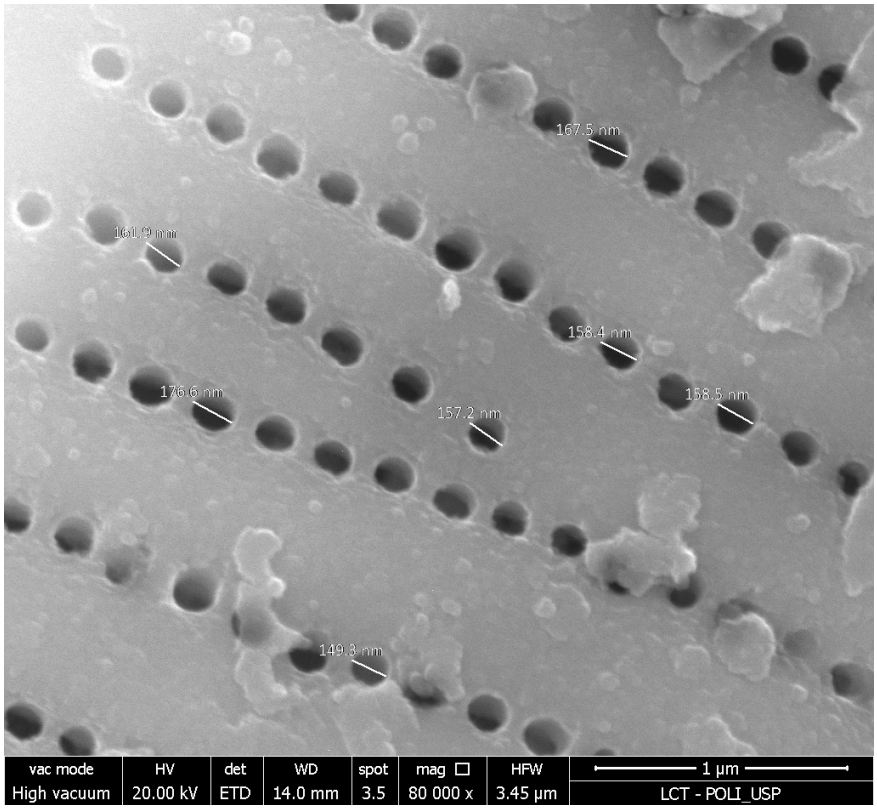

(a)

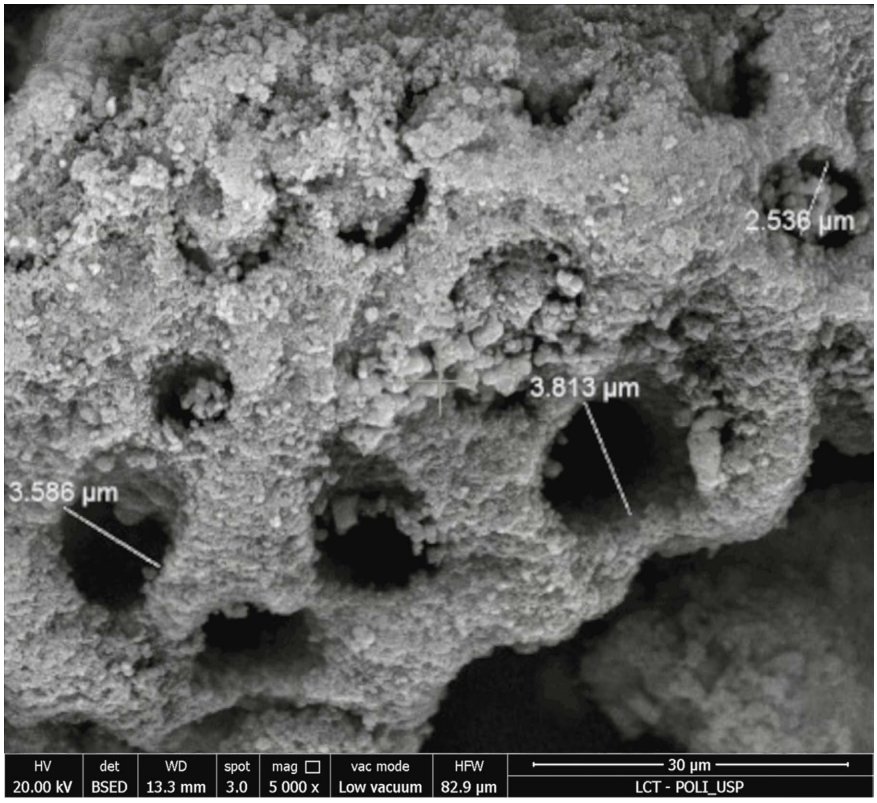

(b)

Figure 1. SEM micrograph of Diatomite (1 µm - (a)) and TiO_2-Diatomite (30 µm - (b)).

The thermogravimetric analysis indicated that the TiO_2-Diatomite exhibited a stable structure. Throughout the observed temperature range, there was no significant mass loss (**Figure 2**).

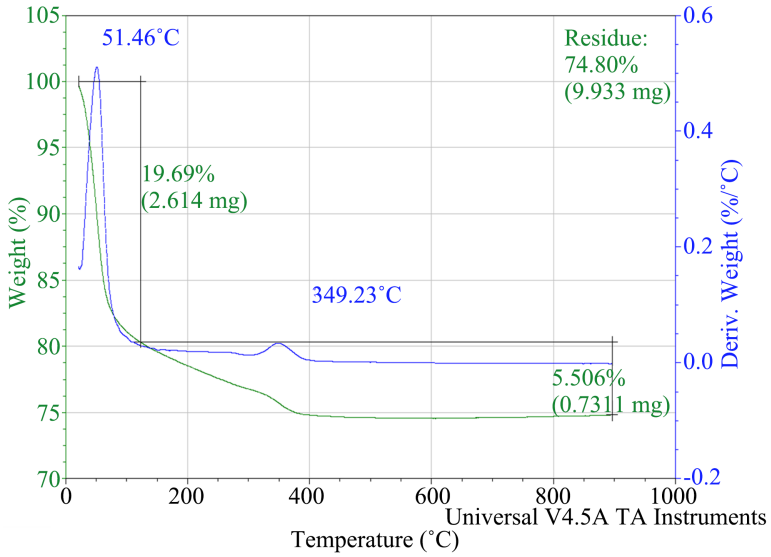

Figure 2. Thermogravimetric analysis (TG-DTA) of TiO_2-Diatomite.

The observed mass loss in the first analysis stage was the adsorbed or absorbed moisture from the material. **Figure 2** shows a weight decrease 19.69% when the temperature reaches 51.46˚C. Subsequently, the material exhibited a second mass loss stage decrease 5.506%, until 400˚C. This temperature represents the morphological change from the anatase crystalline phase to rutile (Zhu et al., 2018). After this stage, the material remained stable until the end of the analysis at 900˚C.

The X-Ray Difratometry (XRD) (**Figure 3**) indicated that the crystalline structure of the material corresponds with the anatase form which is the most suitable structure for photocatalysis. The diffractogram of the TiO_2-Dt material showed diffraction peaks 2θ = 25.26; 37.88; 47.86; 54.06; 62.60; 68.90; 69.70; 75.00 and 82.50.

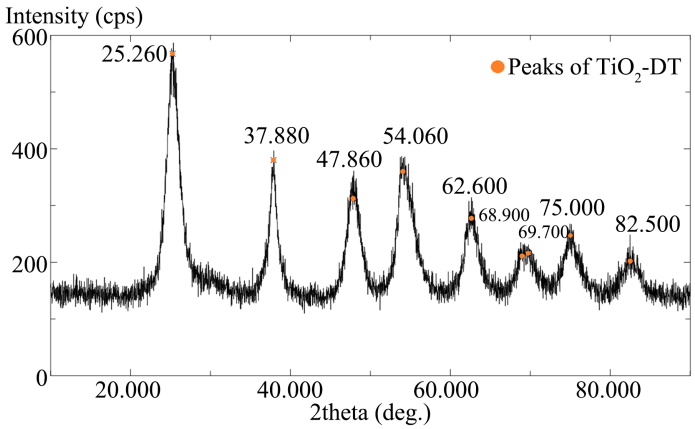

Figure 3. X-ray diffraction pattern of the TiO_2-Dt sample.

In the literature, the description of peaks related to the Anatase form, under the angle of 2θ, are: 25.6; 37.6; 38.2; 48.3; 54.2; 55.6; 63.2; 70.7 and 75.7, indicated by the red dots in **Figure 3** (Najafidoust et al., 2020). By comparing the peaks obtained with the literature, it was possible to identify that the TiO_2 used is in the anatase phase.

3.2. TiO_2-Biocharcoal Characterization

The mass of TiO_2-Biocharcoal obtained during the synthesis was on average 2.8 grams. The surface area was measured by BET analysis and the result was 230 $m^2 \cdot g^{-1}$, this indicates a high surface area due to the size of the particles and their porosity. The value is much higher than the commercial TiO_2 anatase which has a surface area between 45 - 55 $m^2 \cdot g^{-1}$ (Sigma-Aldrich, 2024).

The SEM micrograph presented the TiO_2-Biocharcoal (**Figure 4**) enhanced surface area and microstructure obtained by biotemplate addition in the synthesis of the catalyst. The pores exhibited diameters ranging from 2.7 to 3.1 μm.

The thermogravimetric analysis indicated that the TiO_2-Biocharcoal exhibited a stable structure. Analyzing the mass loss that stands at 19.75%, 13.23% is compatible with the presence of moisture and the loss of 6.60% is related to organic compounds that are part of the synthesis; it is observed that 80.15% of the tested material remained stable between the temperature range and 600˚C to 900˚C, therefore there was no thermal degradation (**Figure 5**).

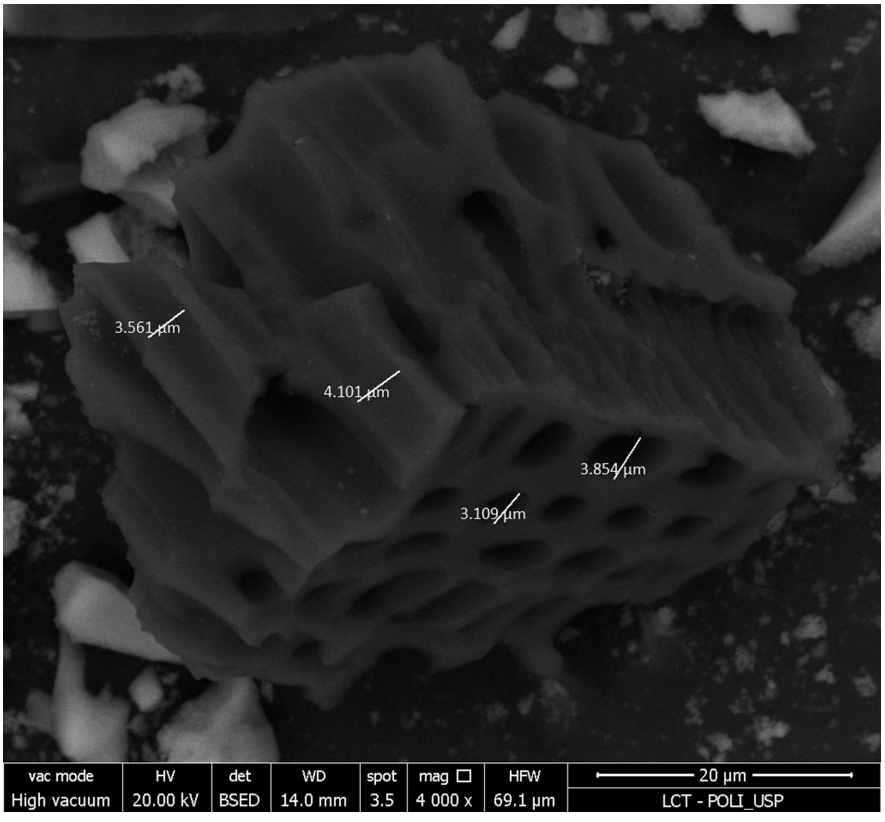

(a)

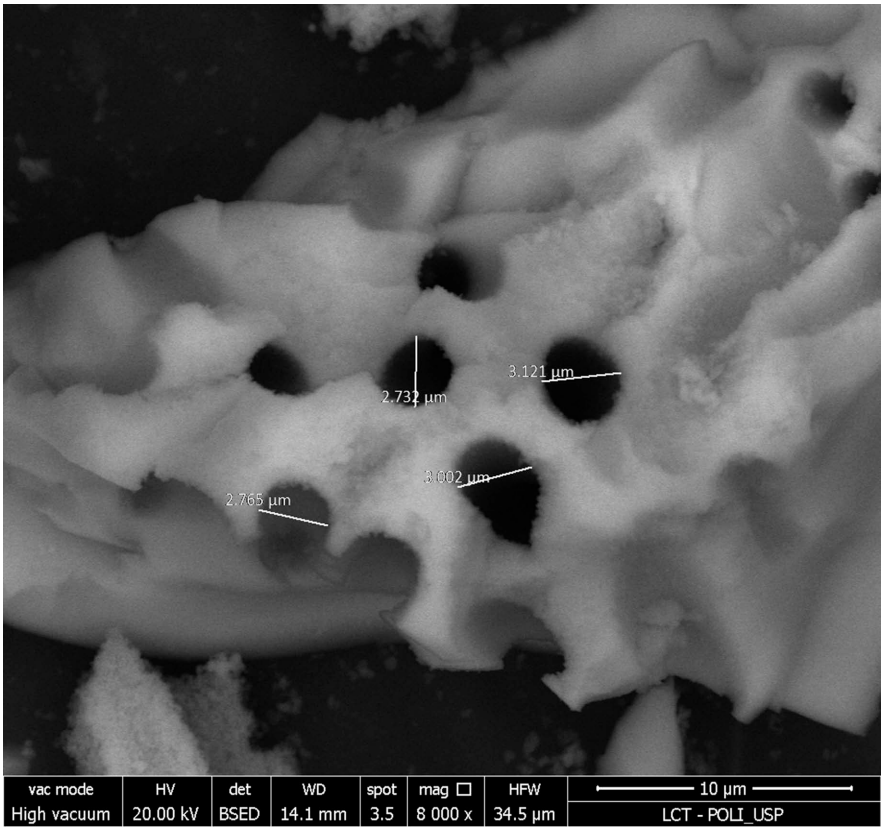

(b)

Figure 4. SEM micrograph of Biocharcoal (20 µm - (a)) and TiO_2-Biocharcoal (10 µm - (b)).

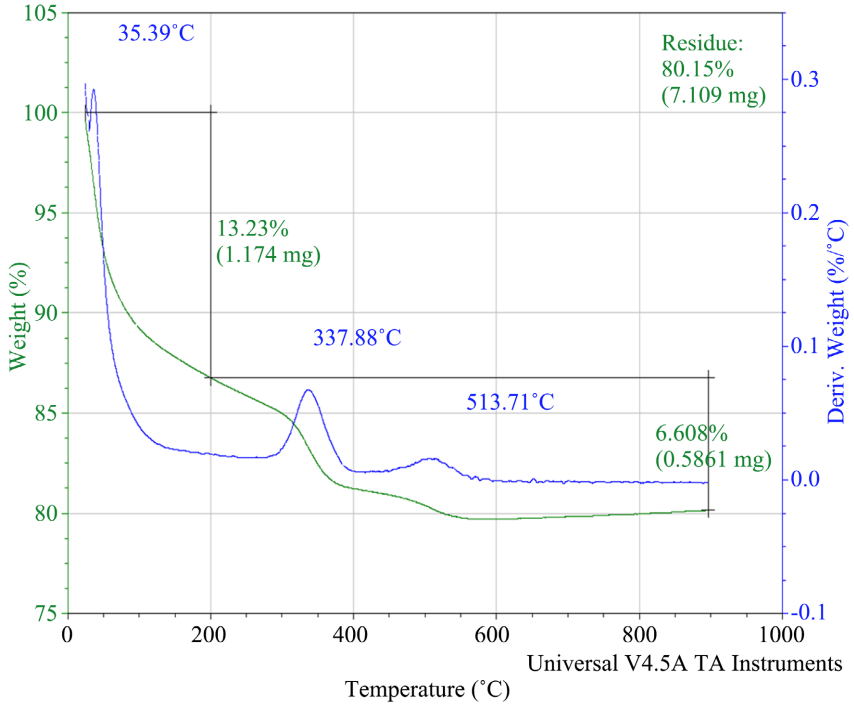

Figure 5. Thermogravimetric analysis (TG-DTA) of TiO_2-Biocharcoal.

The X-Ray Difratometry (XRD) (Figure 6) indicated that the crystalline structure of the material corresponds with the anatase form which is the most suitable structure for photocatalysis. The diffractogram of the TiO_2-BC material showed diffraction peaks 2θ = 25.32; 37.88; 47.92; 54.04; 62.58; 68.80; 69.98; 74.94 and 82.66.

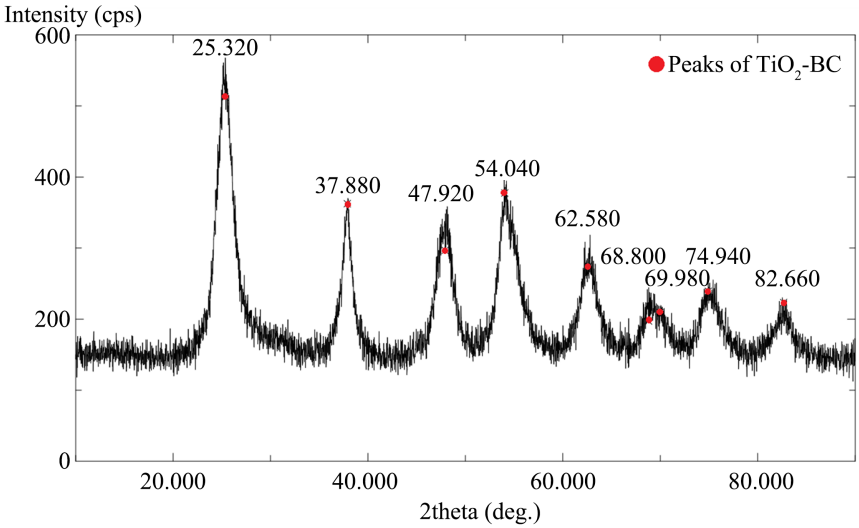

Figure 6. X-ray diffraction pattern of the TiO_2-BC sample.

The X-ray diffractometry was used to confirm the structure of TiO_2-BC. In the literature, the description of peaks related to the Anatase form, under the angle of 2θ, are: 25.6; 37.6; 38.2; 48.3; 54.2; 55.6; 63.2; 70.7 and 75.7, indicated by the red dots in Figure 6 (Najafidoust et al., 2020).

As previously mentioned, there are 3 main crystalline structures presented by the oxide, with anatase being the one with the greatest photocatalytic activity. When analyzing the peaks under the 2Θ angle relating to the test compared to the anatase peaks in the literature, it is noted that they are coincident peaks.

3.3. Photodisinfection Kinetics

All experiments exhibited a disinfection percentage above 96%. Figure 7 shows the colonies on the Petri plates referring to the collections carried out at 0 minutes and 60 minutes of the 2DT experiment, with a total disinfection rate of 99.13%, demonstrating high bacterial inactivation during the process.

Figure 8 shows the colonies on the Petri plates referring to the collections carried out at 0 minutes and 60 minutes of the 3BC experiment, with a total disinfection rate of 98.88%, also demonstrating a high disinfection rate.

Considering the high complexity of the disinfection processes, many references present empirical equations for the kinetic analysis of photocatalytic bacterial inactivation. The Chick-Watson equation (Equation (1)), a disinfection model published in 1908, offers a general expression for such analyses (Watson, 1908).

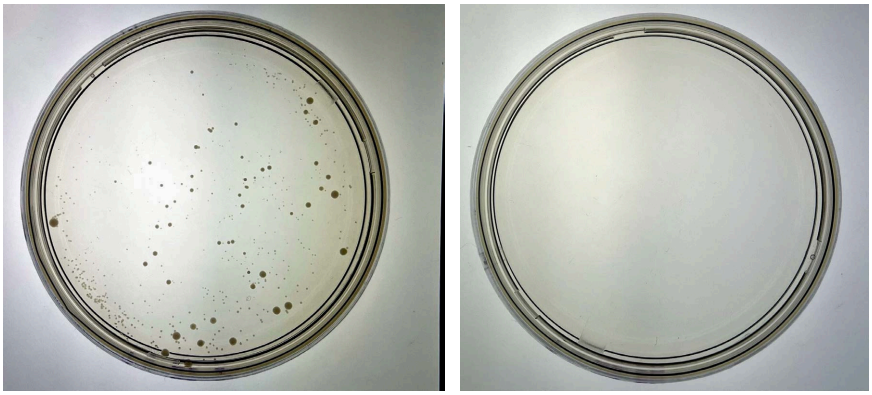

Figure 7. Bacterial inactivation at each collection time (0 and 60 minutes) of the 2DT experiment using 0.5 g·L^{-1} of TiO_2-Diatomite.

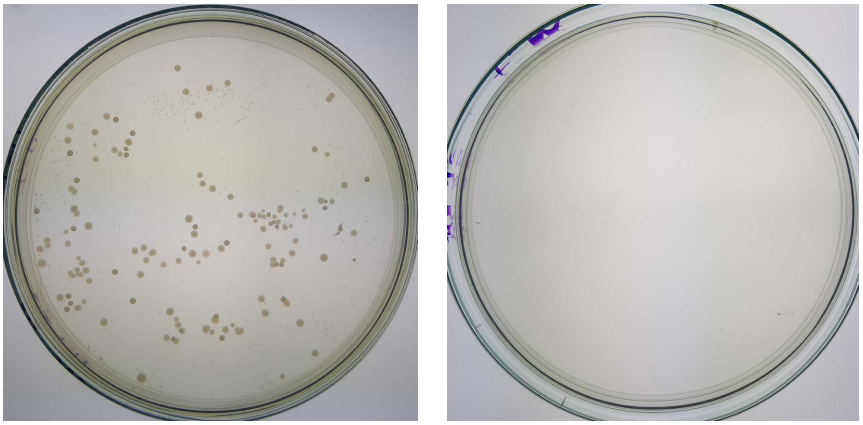

Figure 8. Bacterial inactivation at each collection time (0 and 60 minutes) of the 2BC experiment using 0.5 g·L^{-1} of TiO_2-Biocharcoal.

$$Log\frac{C}{C_0} = -k't \tag{1}$$

where: C/C_0 is the reduction proportion in the bacterial concentration, k is the disinfection kinetic constant at time t.

Some authors attributed the initial delay in the process to a lag stage in the inactivation of the bacteria (Huesca-Espitia et al., 2017). The better representation of such an aspect is the delayed Chick-Watson model to fit the experimental results. This model includes a second parameter called t_0 that corresponds to the time of delay, according to Equation (2):

$$Log\frac{C}{C_0} = \begin{cases} 0, t \le t_0 \\ -k'\left(t - t_0\right), t > t_0 \end{cases} \tag{2}$$

In 1972 the disinfection model proposed by Hom Equation (3) considered a bacterial inactivation with non-linear behavior (Hom, 1972):

$$Log\frac{C}{C_0} = -k't^m \tag{3}$$

The expression incorporates a second parameter called m. When m = 1, the

equation reduces and simplifies to the Chick-Watson linear equation; for $m > 1$, the Hom model reproduces the existence of a shoulder at the beginning of the reaction, whereas, for $m < 1$ the equation permits the fitting of a tail at the end of the process. However, the model cannot reproduce the simultaneous existence of both regions.

For the mathematical study of the kinetic models, the graphs were generated for each equation to determine the kinetic constant (k') of the Chick-Watson model and the parameter (m) of the Hom model. The experiments exposed to LED lamp radiation with TiO_2-Diatomite (1DT, 2DT and 3DT) did not differ from those conducted with TiO_2-Biocharcoal (1BC, 2BC and 3BC). Figure 9 shows correlated experiments with parameter $m < 1$, confirming the presence of a tail in the kinetic graph curve.

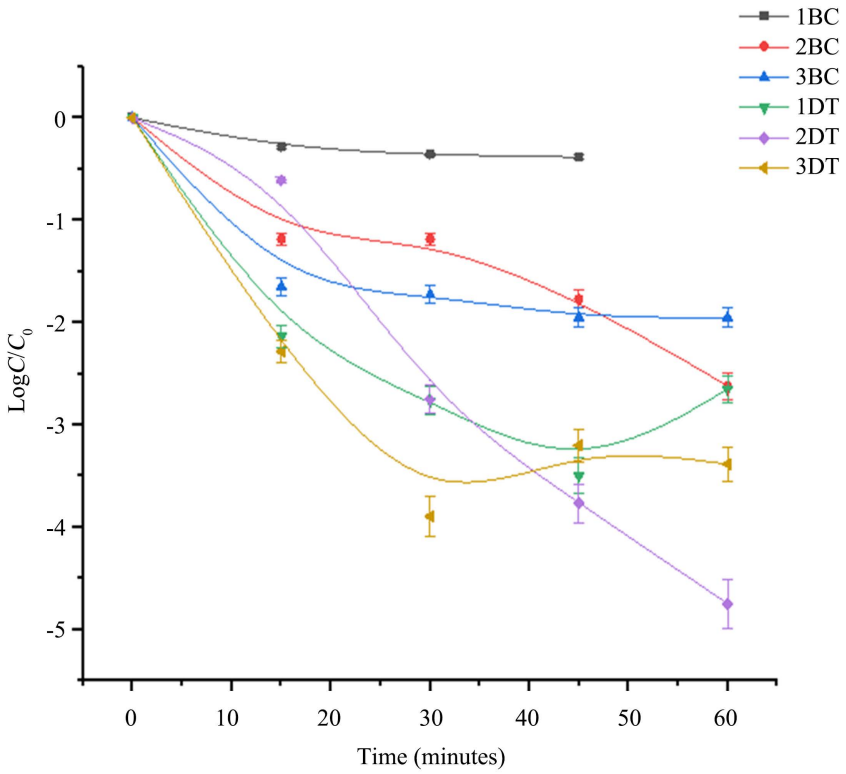

Figure 9. Photodisinfection inactivation of greywater samples in the solar chamber with LED radiation using 0.5 g·L^{-1} TiO_2-Diatomite (1DT, 2DT and 3DT) and 0.5 g·L^{-1} TiO_2-Biocharcoal (1BC, 2BC and 3 BC) and each correlated parameter m.

Experiment 2DT exhibited the highest value of parameter m, indicating the presence of a well-defined shoulder at the beginning of the process (Figure 9—lilac). On the other hand, 3BC had a lower value of m, closer to 0 (Figure 9—blue). Observing Figure 9 in red, there is a reduced shoulder at the beginning, and after 15 minutes, the process approximates the Chick-Watson Modified model with curvy kinetics. The demonstration of all kinetics constants and bacterial inactivation is in Table 3.

Table 3. Photodisinfection inactivation percentage, kinetics constant (k), and parameter m of greywater samples using 0.5 g·L^{-1} TiO_2-Biocharcoal (1BC, 2BC and 3 BC) 0.5 g·L^{-1} and TiO_2-Diatomite (1DT, 2DT and 3DT).

Experiment identification	k' (UFC·mL^{-1}·min^{-1})	m	Bacterial inactivation (%)
1BC	−0.89977	0.043	100
2BC	−7.97522	0.03501	99.76
3BC	−4.49272	0.00503	98.88
1DT	−0.0445	0.02331	96.98
2DT	−0.0843	1.4927	99.13
3DT	−0.0512	0.2593	97.96

According to Sunada et al. (2003), bacterial inactivation occurs due to the cumulative effects of successive attacks by reactive oxygen species (ROS) on the bacterial membrane and cell wall rather than a single attack. Thus, the length of the shoulder region in determining the kinetic inactivation curve is by the rate of ROS generation, influenced by the semiconductor concentration and irradiation flux.

3.4. Toxicity Test

Tests under no radiation demonstrated bacterial growth and stability during the process, indicating that the photocatalysts presented low toxicity for bacterial samples. Figure 10 and Figure 11 confirm that the amount of bacterial colonies remained throughout the process. No significant bacterial inactivation was observed.

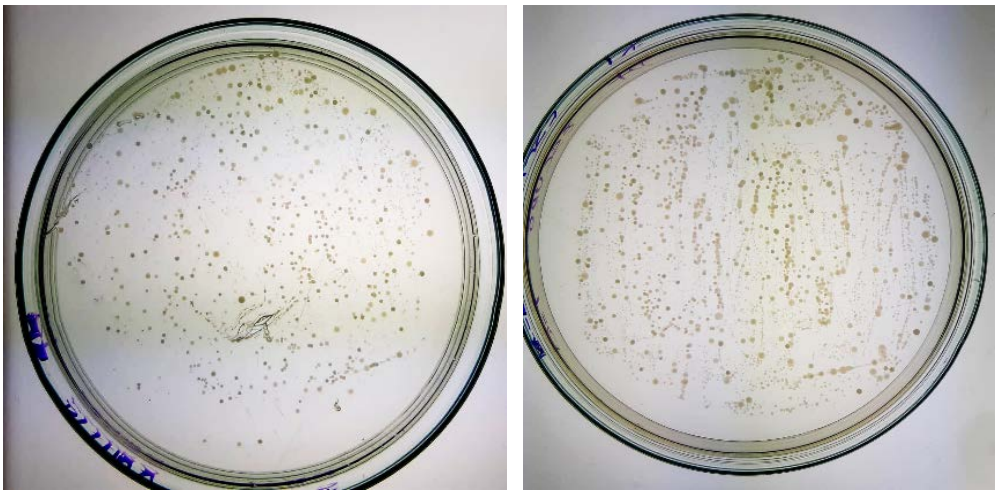

Figure 10. Toxicity test at each collection time (0 and 60 minutes) of the 1DT-tox experiment using 0.5 g·L^{-1} of TiO_2-Diatomite.

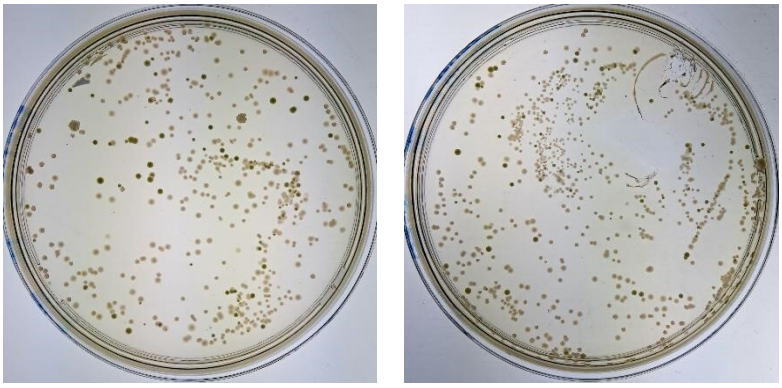

Figure 11. Toxicity test at each collection time (0 and 60 minutes) of the 2BC-tox experiment using 0.5 g·L^{-1} of TiO_2-Biocharcoal.

The Colony-forming unit (CFU) per time for each experiment demonstrated similar behavior indicating a bacterial increase (1BC, 2BC, 3BC and 1DT) and stability (2DT, 3DT) during the process (Figure 12).

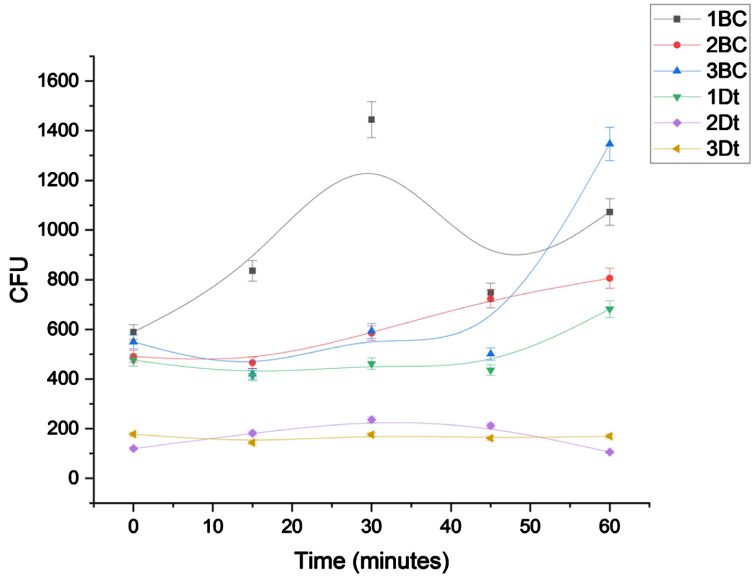

Figure 12. Colony-forming unit (CFU) per minute of greywater samples using 0.5 g·L^{-1} TiO_2-Diatomite (1DT, 2DT and 3DT) and 0.5 g·L^{-1} TiO_2-Biocharcoal (1BC, 2BC and 3 BC) in the solar chamber in the dark (no radiation).

The peak observed at minute 30 of the 1BC tox test refers to a big bacterial growth, then the graph shows a reduction and at the end of the process growth can be observed again. This is due to the fact that microorganisms do not behave in a predictable way, according to the environmental conditions and according to the composition of the sample used. Oscillations in the graph may occur, but the final result defines whether there was a decrease or increase in the number of bacteria colonies compared to the beginning of the process.

No disinfection in the process was observed with the absence of light, confirming the ROS generation stimulated by radiation and a non-reactant material.

4. Conclusion

The experiments conducted with wastewater samples yielded favorable results, with a significant decrease in bacterial colonies after 15 minutes of radiation exposure, resulting in bacterial inactivation above 96%.

The kinetic studies correlated with the Hom model, exhibiting either a tail (assays 1BC, 3BC, 1DT, and 3DT) or a shoulder (2BC and 2DT) in the kinetic curve. In all experiments that displayed a tail, a decrease in the bacterial inactivation rate at the end of the photodisinfection process observed.

The phenomenon of the tail in the kinetic curve is related to the increase in solution turbidity due to the presence of a high number of inactive bacteria at the beginning of the process (15 to 30 minutes), which reduces radiation incidence and, consequently, the production of hydroxyl radicals. Experiments demonstrating a shoulder in the curve indicate a delay in bacterial inactivation. This behavior is associated with the heterogeneity of the collected samples and the high concentration of microorganisms in the medium.

The toxicity tests confirmed that the disinfection is unleashed by radiation. The low toxicity of the photocatalyst towards bacteria present in the rinse water was proven, as the results of tests in absolute darkness showed bacterial growth.

The synthesized TiO_2-Diatomite and TiO_2-Biocharcoal materials demonstrated excellent properties as a photocatalytic disinfection agent in water samples contaminated with bacteria. This study enables the use of abundant renewable sources, such as solar energy in Brazil, for the disinfection of contaminated effluents, employing an accessible material with low toxicity and favorable kinetics.

Further studies aim at identifying and correlating greywater pathogens with photodisinfection kinetics. Additionally, verify not only the purity of disinfected water but also understand the life-cycle of TiO_2 disposal in water bodies. The project proposal envisions the development of an autonomous photodisinfection system for remote areas, sourcing natural solar radiation and applying a material recycling procedure, overcoming economical and ecological obstacles for social and environmental impact.

Acknowledgements

This study was financed by National Council for Scientific and Technological Development (CNPq) processes 131260/2021-0 and 131268/2021-0.

Conflicts of Interest

The authors declare no conflicts of interest regarding the publication of this paper.

References

Bianchi, C. L., Pirola, C., Galli, F., Stucchi, M., Morandi, S., Cerrato, G. et al. (2015). Nano and Micro-TiO_2 for the Photodegradation of Ethanol: Experimental Data and Kinetic

Modelling. *RSC Advances, 5,* 53419-53425. https://doi.org/10.1039/c5ra05385d

Callewaert, C., Van Nevel, S., Kerckhof, F., Granitsiotis, M. S., & Boon, N. (2015). Bacterial Exchange in Household Washing Machines. *Frontiers in Microbiology, 6,* Article 1381. https://doi.org/10.3389/fmicb.2015.01381

Chen, Y., Wu, Q., Wang, J., & Song, Y. (2019). Retracted Article: Visible-Light-Driven Elimination of Oxytetracycline and Escherichia Coli Using Magnetic La-Doped TiO_2/Copper Ferrite/Diatomite Composite. *Environmental Science and Pollution Research, 26,* 26593-26604. https://doi.org/10.1007/s11356-019-05873-w

Coleman, H. M., Marquis, C. P., Scott, J. A., Chin, S. S., & Amal, R. (2005). Bactericidal Effects of Titanium Dioxide-Based Photocatalysts. *Chemical Engineering Journal, 113,* 55-63. https://doi.org/10.1016/j.cej.2005.07.015

Huesca-Espitia, L. L. D. C., Aurioles-Lopez, V., Ramirez, I., Sánchez-Salas, J. L., Bandala, E. R. (2017). Photocatalytic Inactivation of Highly Resistant Microorganisms in Water: A Kinetic Approach. *Journal of Photochemistry and Photobiology A: Chemistry, 337,* 132-139. https://doi.org/10.1016/j.jphotochem.2017.01.025

Fawzi, T., Rani, S., Roy, S. C., & Lee, H. (2022). Photocatalytic Carbon Dioxide Conversion by Structurally and Materially Modified Titanium Dioxide Nanostructures. *International Journal of Molecular Sciences, 23,* Article 8143. https://doi.org/10.3390/ijms23158143

Ganguly, P., Byrne, C., Breen, A., & Pillai, S. C. (2018). Antimicrobial Activity of Photocatalysts: Fundamentals, Mechanisms, Kinetics and Recent Advances. *Applied Catalysis B: Environmental, 225,* 51-75. https://doi.org/10.1016/j.apcatb.2017.11.018

Gattlen, J., Amberg, C., Zinn, M., & Mauclaire, L. (2010). Biofilms Isolated from Washing Machines from Three Continents and Their Tolerance to a Standard Detergent. *Biofouling, 26,* 873-882. https://doi.org/10.1080/08927014.2010.524297

Geissmann, Q. (2013). Opencfu, a New Free and Open-Source Software to Count Cell Colonies and Other Circular Objects. *PLOS ONE, 8,* e54072. https://doi.org/10.1371/journal.pone.0054072

Gopal, K., Tripathy, S. S., Bersillon, J. L., & Dubey, S. P. (2007). Chlorination Byproducts, Their Toxicodynamics and Removal from Drinking Water. *Journal of Hazardous Materials, 140,* 1-6. https://doi.org/10.1016/j.jhazmat.2006.10.063

Hom, L. W. (1972). Kinetics of Chlorine Disinfection in an Ecosystem. *Journal of the Sanitary Engineering Division, 98,* 183-194. https://doi.org/10.1061/jsedai.0001370

Intergovernmental Panel on Climate Change (IPCC) (2023). *Synthesis Report of the IPCC Sixth Assessment Report (AR6).* https://www.ipcc.ch/report/ar6/syr/>

Levy, K., Smith, S. M., & Carlton, E. J. (2018). Climate Change Impacts on Waterborne Diseases: Moving toward Designing Interventions. *Current Environmental Health Reports, 5,* 272-282. https://doi.org/10.1007/s40572-018-0199-7

Marugán, J., van Grieken, R., Pablos, C., Satuf, M. L., Cassano, A. E., & Alfano, O. M. (2011). Rigorous Kinetic Modelling with Explicit Radiation Absorption Effects of the Photocatalytic Inactivation of Bacteria in Water Using Suspended Titanium Dioxide. *Applied Catalysis B: Environmental, 102,* 404-416. https://doi.org/10.1016/j.apcatb.2010.12.012

Marugán, J., van Grieken, R., Sordo, C., & Cruz, C. (2008). Kinetics of the Photocatalytic Disinfection of *Escherichia coli* Suspensions. *Applied Catalysis B: Environmental, 82,* 27-36. https://doi.org/10.1016/j.apcatb.2008.01.002

Matsunaga, T., Tomoda, R., Nakajima, T., & Wake, H. (1985). Photoelectrochemical Sterilization of Microbial-Cells by Semiconductor Powders. *FEMS Microbiology Letters,*

29, 211-214.

Mesones, S., Mena, E., López-Muñoz, M. J., Adán, C., & Marugán, J. (2020). Synergistic and Antagonistic Effects in the Photoelectrocatalytic Disinfection of Water with TiO_2 Supported on Activated Carbon as a Bipolar Electrode in a Novel 3D Photoelectrochemical Reactor. *Separation and Purification Technology, 247,* Article ID: 117002. https://doi.org/10.1016/j.seppur.2020.117002

Najafidoust, A., Allahyari, S., Rahemi, N., & Tasbihi, M. (2020). Uniform Coating of TiO_2 Nanoparticles Using Biotemplates for Photocatalytic Wastewater Treatment. *Ceramics International, 46,* 4707-4719. https://doi.org/10.1016/j.ceramint.2019.10.202

Ortega-Gómez, E., Esteban García, B., Ballesteros Martín, M. M., Fernández Ibáñez, P., & Sánchez Pérez, J. A. (2013). Inactivation of Enterococcus Faecalis in Simulated Wastewater Treatment Plant Effluent by Solar Photo-Fenton at Initial Neutral Ph. *Catalysis Today, 209,* 195-200. https://www.sciencedirect.com/science/article/pii/S0920586113000795 https://doi.org/10.1016/j.cattod.2013.03.001

Ortiz, N., Silva, A., Lima, G. N. S., & Hyppolito, F. P. (2018). Using Solar-TiO_2 and Biocarbon to Decompose and Adsorb Amoxicillin from Polluted Waters. *International Journal of Chemistry, 10,* Article 131. https://doi.org/10.5539/ijc.v10n1p131

Shimizu, Y., Ateia, M., Wang, M., Awfa, D., & Yoshimura, C. (2019). Disinfection Mechanism of *E. coli* by CNT-TiO_2 Composites: Photocatalytic Inactivation vs. Physical Separation. *Chemosphere, 235,* 1041-1049. https://doi.org/10.1016/j.chemosphere.2019.07.006

Sigma-Aldrich (2024). *Product Specification.* Titanium (IV) Dioxide, Anatase Nano-Powder. https://www.sigmaaldrich.com/specification-sheets/440/011/637254-BULK_____ALDRICH__.pdf

Sunada, K., Watanabe, T., & Hashimoto, K. (2003). Studies on Photokilling of Bacteria on TiO_2 Thin Film. *Journal of Photochemistry and Photobiology A: Chemistry, 156,* 227-233. https://doi.org/10.1016/s1010-6030(02)00434-3

Tortora, G. J., Case, C. L., & Funke, B. R. (2016). *Microbiology: An Introduction* (12th ed.). Pearson.

Trazzi, P. A., Higa, A. R., Dieckow, J., Mangrich, A. S., & Higa, R. C. V. (2018). Biocarvão: Realidade e potencial de uso no meio florestal. *Ciência Florestal, 28,* 875-887. https://doi.org/10.5902/1980509832128

United Nations Children's Fund (UNICEF) & World Health Organization (2021). *Progress on Household Drinking Water, Sanitation and Hygiene/2000-2020: Five Years into the SDGs.*

United Nations Development Group (UNDG) (2016). *The Sustainable Development Goals (SDGs) Are Coming.* High Level Political Forum (HLPF).

Wang, S., Lian, J. S., Zheng, W. T., & Jiang, Q. (2012). Photocatalytic Property of Fe Doped Anatase and Rutile TiO_2 Nanocrystal Particles Prepared by Sol-Gel Technique. *Applied Surface Science, 263,* 260-265. https://doi.org/10.1016/j.apsusc.2012.09.040

Watson, H. E. (1908). A Note on the Variation of the Rate of Disinfection with Change in the Concentration of the Disinfectant. *Epidemiology and Infection, 8,* 536-542. https://doi.org/10.1017/s0022172400015928

Wu, Y., Li, X., Yang, Q., Wang, D., Xu, Q., Yao, F. et al. (2019). Hydrated Lanthanum Oxide-Modified Diatomite as Highly Efficient Adsorbent for Low-Concentration Phosphate Removal from Secondary Effluents. *Journal of Environmental Management, 231,* 370-379. https://doi.org/10.1016/j.jenvman.2018.10.059

Zhu, X., Han, S., Feng, W., Kong, Q., Dong, Z., Wang, C. et al. (2018). The Effect of Heat Treatment on the Anatase-Rutile Phase Transformation and Photocatalytic Activity of Sn-Doped TiO_2 Nanomaterials. *RSC Advances, 8,* 14249-14257. https://doi.org/10.1039/c8ra00766g